

Postprint Version

G. McHale, R. Lücklum, M.I. Newton and J.A. Cowen, *Influence of viscoelasticity and interfacial slip on acoustic wave sensors*, J. Appl. Phys., **88** 7304-7312 (2000); DOI:10.1063/1.1326855.

The following article appeared in [Journal of Applied Physics](http://link.aip.org/link/?JAPIAU/88/7304/1) and may be found at <http://link.aip.org/link/?JAPIAU/88/7304/1>. Copyright ©2000 American Institute of Physics.

File reconstructed from Pre-print file: May not be the final version.

Influence of Viscoelasticity and Interfacial Slip on Acoustic Wave Sensors

G. McHale^{**}, R. Lucklum[‡], M.I. Newton^{*} and J.A. Cowen^{*}

^{*}Department of Chemistry and Physics, The Nottingham Trent University, Clifton Lane, Nottingham NG11 8NS, UK.

[‡]Institute for Micro- and Sensor Systems, Faculty of Electrical Engineering and Information Technology, Otto-von-Guericke University, P.O.B. 4120, D-39016 Magdeburg, Germany.

^{*} email: glen.mchale@ntu.ac.uk; Tel: +44 115 848383; Fax: +44 115 9486636

Abstract

Acoustic wave devices with shear horizontal displacements, such as quartz crystal microbalances (QCM) and shear horizontally polarised surface acoustic wave (SH-SAW) devices provide sensitive probes of changes at solid-solid and solid-liquid interfaces. Increasingly the surfaces of acoustic wave devices are being chemically or physically modified to alter surface adhesion or coated with one or more layers to amplify their response to any change of mass or material properties. In this work, we describe a model that provides a unified view of the modification in the shear motion in acoustic wave systems by multiple finite thickness loadings of viscoelastic fluids. This model encompasses QCM and other classes of acoustic wave devices based on a shear motion of the substrate surface and is also valid whether the coating film has a liquid or solid character. As a specific example, the transition of a coating from liquid to solid is modelled using a single relaxation time Maxwell model. The correspondence between parameters from this physical model and parameters from alternative acoustic impedance models is given explicitly. The characteristic changes in QCM frequency and attenuation as a function of thickness are illustrated for a single layer device as the coating is varied from liquid-like to that of an amorphous solid. Results for a double layer structure are given explicitly and the extension of the physical model to multiple layers is described. An advantage of this physical approach to modelling the response of acoustic wave devices to multilayer films is that it provides a basis for considering how interfacial slip boundary conditions might be incorporated into the acoustic impedance used within circuit models of acoustic wave devices. Explicit results are derived for interfacial slip occurring at the substrate-layer 1 interface using a single real slip parameter, s , which has inverse dimensions of impedance. In terms of acoustic impedance, such interfacial slip acts as a single-loop negative feedback. It is suggested that these results can also be viewed as arising from a double-layer model with an infinitesimally thin slip layer which gives rise to a modified acoustic load of the second layer. Finally, the difficulties with defining appropriate slip boundary conditions between any two successive layers in a multilayer device are outlined from a physical point of view.

Keywords: Acoustic waves, quartz crystal microbalances, sensors, slip, contact angles, wetting.

I. Introduction

Acoustic wave devices provide a simple and effective means for probing changes at the interface between a solid film or a liquid. An example of such a device is the quartz crystal microbalance (QCM) which uses a transverse-shear mode oscillation. Sauerbrey¹ showed that the decrease in resonant frequency of the device due to loading the surface by a thin film of a rigidly coupled material is proportional to the mass (change) of the film, Δm , and to the square of the frequency, f . In this case, no change in damping of the resonance occurs and so only an energy storage is occurring. When a QCM is operated in a liquid the oscillation of the device surface is coupled into the liquid and induces an oscillation in the liquid. This oscillation does not extend throughout the bulk of the liquid, but is damped within a small distance, $\delta = (2\eta_f / \omega\rho_f)^{1/2}$ where η_f is the viscosity, ρ_f is the density and $\omega = 2\pi f$ is the angular frequency. As a consequence of this viscous entrainment of the liquid, the frequency decrease is related to the square root of the density viscosity product and to a lower power of the frequency^{2,3}, $f^{3/2}$. In addition, a damping of the QCM resonance, also related to the square root of the density viscosity product occurs indicating that energy loss is occurring.

In recent years, the application of acoustic wave devices has been extended to include *in-situ* monitoring of film deposition, e.g. in electrochemistry^{4,5}, and chemical and biological sensing, e.g. sensing with polymer coated devices⁶⁻⁹. A common feature of these applications is that the device surfaces are coated with materials that are neither purely rigidly coupled mass nor simply Newtonian type liquids. It has therefore become essential that models of acoustic device response to layers of viscoelastic materials be developed. Moreover, these models need to allow for multiple and finite thickness coatings and operation of devices in liquid. A general approach is to consider the acoustic impedance, Z_L , at the interface between the acoustic device and the coating. This surface acoustic impedance summarizes the overall acoustic load acting on the acoustic device and can be applied to single and multilayer arrangements¹⁰. With some approximations, this model can be translated into equivalent

circuit models used in electrical engineering¹¹⁻¹³. *The imaginary part of the impedance gives the frequency shift and the real part gives the damping.* An alternative approach, applied to the change in response of a QCM due to a Newtonian liquid, was developed by Rodahl and Kasemo¹⁴. They considered the motion of the unloaded QCM surface to be a damped simple harmonic oscillator and then deduced the increase in damping due to shear stress on the surface arising from immersion in a liquid. They have recently extended this theory to two polymer layers with the viscoelastic material modelled as a Voigt element¹⁵. McHale *et al*¹⁶ have also considered the extension of the simple harmonic oscillator model to include a single polymer layer, but using a Maxwell model for the viscoelasticity and allowing for a range of acoustic wave devices. An implication of this extension is that the results of the simple harmonic oscillator model are valid not only for QCM devices, but also all classes of acoustic wave devices based on shearing of the surface loadings. This alternative physical approach to modelling acoustic wave device response has the advantage of providing access to the physical boundary conditions.

One aspect of QCM response that has generated controversy is the possible role of interfacial slip. It appears clear from the work of Krim *et al*^{17,18} that when certain atoms are adsorbed onto the surface of a QCM in ultra high vacuum conditions they can lock together as the layer coverage approaches a monolayer and slide on the surface. However, whether slip occurs when a QCM is operated in a liquid or with a polymer coating is far less certain. Several authors have reported an apparent dependence of the acoustic impedance on the contact angle of the liquid, and hence surface wettability¹⁹⁻²¹. Martin *et al*^{22,23} have argued that apparently anomalous results for the acoustic impedance can arise from surface roughness. The argument is that air or liquid can be trapped within small pits on a device surface. Trapped liquid could act as a rigid mass loading in the Sauerbrey manner while trapped air prevents such a mechanism. This would distort the response that would be expected if only viscous entrainment, in the Kanazawa and Gordon manner, occurred. Contact angle dependence then arises in the acoustic response as liquid penetration into small surface aspherities and is

determined by surface wettability. Whilst it is clear air trapping could occur, it is not clear that all anomalies in measured acoustic impedances are due to this mechanism. An obvious alternative mechanism for anomalous acoustic response that could depend on interfacial energy is slip. It is anticipated that should slip be a mechanism influencing QCM response it could have its greatest impact in biological sensor applications where the hydrophobicity and hydrophilicity of the interface may change.

A particular difficulty in assessing whether slip is occurring when QCM devices are operated in liquids is that few models exist that can predict how device response would be altered. Such models need to be sufficiently flexible to allow for both bare devices operated in liquid and for coated devices. Whilst circuit models of QCM response are useful, and can be extended to multiple viscoelastic layers, they do not offer a simple and transparent way of including interfacial slip. Hayward and Thompson^{24,25} have presented a model that included both interfacial slip and multiple viscoelastic layers. However, the inclusion of slip involved complex slip parameters that were not explicitly related to the impedance of the layers.

In this work, we first review the physical model¹⁶ of acoustic wave device response with a single viscoelastic layer. Previously presented expressions are reformulated in the form of the general complex shear modulus and the acoustic impedance, since it is this impedance which is often most directly related to the values measured in experiments (Section IIa). The model is then extended to include multiple viscoelastic layers and so provide a simple, but general, framework in which to consider interfacial slip (Section IIb). The no-slip boundary condition at the device-viscoelastic first layer interface is then relaxed using a Stokes friction law, as previously suggested for a QCM in contact with a Newtonian fluid¹⁴. This boundary condition introduces a single real slip parameter, s , and results in a simple recipe for the inclusion of slip in the response of any acoustic wave device based on shearing motion induced in viscoelastic layers (Section IIc). The physical significance of the slip parameter is discussed and an acoustic load concept is introduced as an interpretation of interfacial slip in a single layer

device. Finally, boundary conditions for slip occurring at the interface between any two layers in a multiple layer device are considered.

II. Theory

IIa. Single layer and no slip

Experimental measurements can involve oscillators measuring the frequency shift and electrical amplification to compensate damping, configurations measuring the damping of an oscillation following excitation at the resonant frequency or impedance analysers measuring the complex electrical impedance. It is therefore useful to note that in sensor applications changes in (angular) frequency, $\Delta\omega$, acoustic energy dissipation, ΔD , and electrical impedance, Z , are caused by surface mechanical impedance (or acoustic load) changes. The surface mechanical impedance of the film, Z_L , can be defined by,

$$Z_L = \frac{F_f}{\dot{q}_s} \quad (1)$$

In a linear approximation these relations for a QCM are given by,

$$\Delta\omega = \frac{-1}{\rho_q t_q} \text{Im} \left[\frac{F_f}{\dot{q}_s} \right] = \frac{-1}{\rho_q t_q} \text{Im}[Z_L] \quad (2)$$

and

$$\Delta D = \frac{2}{\omega \rho_q t_q} \text{Re} \left[\frac{F_f}{\dot{q}_s} \right] = \frac{2}{\omega \rho_q t_q} \text{Re}[Z_L] \quad (3)$$

where ρ_q and t_q are the density and thickness of the substrate. Eqs. (2) and (3) can be derived within the damped simple harmonic oscillator model. In terms of a QCM the surface impedance is related to the quartz substrate parameters by,

$$\Delta Z = \frac{1}{\omega C_0} \frac{\alpha_q}{4K^2 Z_q} Z_L \quad (4)$$

where Z_q and acoustic impedance of the quartz substrate, α_q is the wave phase shift in the quartz substrate and K is a value of electromechanical coupling^{10,26,27} F_f is the force exerted by

the film on the quartz substrate per unit area and \dot{q}_s is the speed of displacement of the quartz substrate¹⁴. In this paper, we will use the real part of the impedance and dissipation or energy loss as interchangeable terminology. Similarly, the imaginary part of the impedance will also be referred to as frequency shift or energy storage.

To evaluate the force exerted by a Newtonian liquid on the substrate it is necessary to obtain a profile of fluid flow by solving the Navier-Stokes equations for a viscous and incompressible fluid. This approach can be extended to other classes of acoustic wave devices by replacing the quartz density by the substrate density, ρ_s , and the quartz thickness t_q by $\xi\lambda$ where λ is the acoustic wavelength in the (unloaded) substrate and ξ is a parameter representing the depth of substrate oscillating¹⁶. For a QCM $\xi=1/2$ and for a shear horizontal surface acoustic wave (SH-SAW) $\xi=1$. Fig. 1 shows the relative direction of oscillations for a QCM, a SH-SAW and the in-plane component of a Rayleigh acoustic wave (SAW). For a SH-SAW or SAW propagating along a path covered by a fluid Eq. 3 can be replaced by a loss per unit length, L of

$$L = \frac{-20\omega(\log_{10} e)}{\rho_s \xi v} \operatorname{Re} \left[\frac{F_f}{\dot{q}_s} \right] \quad (5)$$

where v is the (unloaded) speed of the acoustic wave.

In our previous works we included viscoelasticity in the model by a complex shear modulus, G_f , or by modifying the Navier-Stokes equations and the equation for the shear stress in the fluid. The equation for fluid flow is then,

$$i\omega \underline{v}_f = \frac{G_f}{i\omega \rho_f} \nabla^2 \underline{v}_f \quad (6)$$

where ρ_f is the density of the fluid, \underline{v}_f is the fluid velocity, and a time dependence $e^{i\omega t}$ has been assumed. Eq. (6) is the wave equation for bulk shear waves propagating in a viscoelastic medium and a solution can be found using the velocity profiles,

$$\text{QCM} \quad \underline{v}_f = (v_f(z)e^{i\omega t}, 0, 0) \quad (7)$$

$$\text{SH-SAW} \quad \underline{v}_f = (0, v_f(z)e^{i(\omega t - kx)}, 0) \quad (8)$$

$$\text{SAW} \quad \underline{v}_f = (v_f(z)e^{i(\omega t - kx)}, 0, u_f(z)e^{i(\omega t - kx)}) \quad (9)$$

and the two boundary conditions,

$$v_f(z=0) = \dot{q}_s \quad (10)$$

and

$$\frac{G_f}{i\omega} \left(\frac{\partial v_f}{\partial z} + \frac{\partial u_f}{\partial x} \right)_{z=t_f} = 0 \quad (11)$$

Eq. (10) is the no-slip condition at the film-substrate interface and Eq. (11) is the continuity of shear stress at the free surface of the film, which is of thickness t_f . The solution for the fluid speed $v_f(z)$ is identical for all three types of device provided $v_{sh}^2 \ll v^2$, where v_{sh} is the shear speed of the film, and is given by,

$$v_f(z) = \dot{q}_s \left\{ \frac{\cosh \left[\sqrt{\frac{-2\omega\eta_f}{G_f \delta}} (z - t_f) \right]}{\cosh \left[\sqrt{\frac{-2\omega\eta_f}{G_f \delta}} t_f \right]} \right\} \quad (12)$$

The corresponding impedance is then given by,

$$Z_f = \sqrt{\rho_f G_f} \tanh \left[i\omega t_f \sqrt{\frac{\rho_f}{G_f}} \right] \quad (13)$$

which is exactly the same result as derived from the transmission line model for the acoustic load of a single (viscoelastic) film.^{10,13}

The Maxwell model for viscoelasticity views the total rate of strain as a spring and a dashpot connected in series. The complex shear modulus is then,

$$G_f = \frac{i\omega\eta_f}{1 + i\omega\tau} \quad (14)$$

where $\tau = \eta_f / \mu_f$ is the relaxation time, and μ_f is the high frequency shear modulus. In the notation of Behling^{26,27}, $\omega\tau = 1/\kappa$ where κ is the loss factor of the polymer and is the ratio of the viscous to elastic contributions to the shear modulus. The Maxwell model contains the limits of Newtonian liquids and rigid solid overlayers and so the theory can represent a large number of device configurations that are relevant to sensing applications. In this formulation we can define a complex effective penetration depth, $\bar{\delta}$, of,

$$\bar{\delta} = \frac{\delta}{\sqrt{1 + i\omega\tau}} \quad (15)$$

which gives more physically obvious forms for the fluid speed,

$$v_f(z) = \dot{q}_s \left\{ \frac{\cosh\left[\frac{\sqrt{2i}(z - t_f)}{\bar{\delta}}\right]}{\cosh\left[\frac{\sqrt{2it_f}}{\bar{\delta}}\right]} \right\} \quad (16)$$

and the film impedance,

$$Z_f = \left(\frac{\bar{\delta}}{\delta}\right) \sqrt{i\omega\rho_f\eta_f} \tanh\left[\frac{\sqrt{2it_f}}{\bar{\delta}}\right] \quad (17)$$

Iib. Multiple layers and no slip

Model definition

In the case of an acoustic wave device with n multiple layers of thickness t_k , we simplify solve the general problem by assuming that $v_{shk}^2 \ll v^2$, where v_{shk} is the shear wave speed in any one layer. The oscillation in each layer induced by the substrate motion will satisfy the equivalent of Eq. (6),

$$i\omega v_k(z) = \frac{G_k}{i\omega\rho_k} \frac{d^2 v_k(z)}{dz^2} \quad (18)$$

where ρ_k is the density of the layer k and G_k is the complex shear modulus of the layer. The general solution for each layer is then of the form,

$$v_k(z) = \dot{q}_s \left[A_k e^{\alpha_k z} + B_k e^{-\alpha_k z} \right] \quad (19)$$

where,

$$\alpha_k^2 = -\frac{\omega^2 \rho_k}{G_k} \quad (20)$$

To obtain specific solutions it is necessary to impose boundary conditions at the interface between the substrate and the first layer, all intermediate interfaces and at the free surface of the top most layer. Assuming no-slip the appropriate boundary conditions are,

$$v_1(z=0) = \dot{q}_s \quad (21)$$

$$v_k\left(\sum_{p=1}^k t_p\right) = v_{k+1}\left(\sum_{p=1}^k t_p\right) \quad (22)$$

$$G_k \left[\frac{dv_k}{dz} \right]_{z=\sum_{p=1}^k t_p} = G_{k+1} \left[\frac{dv_{k+1}}{dz} \right]_{z=\sum_{p=1}^k t_p} \quad (23)$$

$$G_n \left[\frac{dv_n}{dz} \right]_{z=\sum_{p=1}^n t_p} = 0 \quad (24)$$

Eqs. (22) and (23) represent a set of equations with $k=1$ to $n-1$ and the summations simply define the z location of the relevant interface. The acoustic impedance presented to the substrate by the combined overlayers is given by the shear stress acting at the substrate-first layer interface,

$$Z_f = \frac{F_f}{\dot{q}_s} = \frac{-G_1}{i\omega\dot{q}_s} \left(\frac{dv_1}{dz} \right)_{z=0} \quad (25)$$

In the no-slip case, Z_f is related to the first coefficient in the solution, Eq. (19), through the factor $2A_1-1$. Eqs. (19)-(25) define the problem for the acoustic impedance for an arbitrary number of finite thickness viscoelastic layers. Solving these equations enables the calculation of energy storage and energy loss due to shearing motion induced in the viscoelastic overlayers by a range of acoustic wave devices. The transmission line model relates the overall acoustic impedance of a multilayer arrangement to the surface acoustic impedance at the device-first film interface with a chain matrix technique^{10,13}, starting from the front

acoustic port. The acoustic impedance for the k -th layer with the acoustic load, Z_{k+1} , at the outer surface is²⁸:

$$Z_k = Z_{ck} \frac{Z_{k+1} + jZ_{ck} \tan(\omega(\rho_k/Z_{ck})t_k)}{Z_{ck} + jZ_{k+1} \tan(\omega(\rho_k/Z_{ck})t_k)} \quad (26)$$

where $Z_{ck} = \sqrt{\rho_k G_k}$ is the characteristic acoustic impedance of the k^{th} layer. The impedance calculated for $k = 1$ is the surface acoustic load impedance, Z_L .

Solution for two layers

It is useful to obtain the analytical solution for a system with two arbitrary thickness overlayers so that the consistency of the method can be verified. After some algebra we find,

$$Z_L = \left(\frac{Z_1 + Z_2}{1 + \frac{Z_1 Z_2}{\rho_1 G_1}} \right) \quad (27)$$

where

$$Z_k = \sqrt{\rho_k G_k} \tanh\left(i\omega t_k \sqrt{\frac{\rho_k}{G_k}}\right) \quad k=1,2 \quad (28)$$

is the acoustic impedance of each individual film. Within the Maxwell model, the relationship to a fluid-like layer can be made more obvious by using the analogous relation to Eq. (17), which explicitly introduces a viscous penetration depth through $\alpha_k = \sqrt{2i/\delta_k}$. Eqs. (27) and (28) agree with results from transmission line models²⁷. In general, the total acoustic impedance for a multilayer system is not simply the sum of the individual impedances of each layer (Eq. (28)). Lucklum *et al*^{29,30} have discussed how the existence of the denominator in Eq. (27) can be used to obtain amplification in sensors by making the first layer a rubbery polymer.

IIIc. Slip boundary condition

Device-layer one interface

One difficulty with the transmission line approach to modelling the acoustic impedance is that the method for inclusion of slip at interfaces is not obvious. The transmission line model assumes continuity of mechanical tension and particle velocity. With the physical model interfacial-slip can be accounted for by altering the boundary conditions, eqs. (21)-(24), in the solution for the motion of the layers. In the model for Newtonian fluids on QCM's, Rodahl and Kasemo¹³, argued that slip at the device interface could be related to the shear stress acting on the substrate due to the liquid. They invoked a Stokes law and suggested that Eq. (21) be replaced by,

$$\chi m_{ML} (\dot{q}_s - v_1(z=0)) = F_f \quad (29)$$

where χ is the coefficient of friction between the film and the surface and m_{ML} is the mass per unit area of a monolayer of the film. Within the context of viscoelastic layers of finite thickness we replace the factor of χm_{ML} occurring in Eq. (29) by a single real parameter $1/s_1$. Applying this boundary condition to a multilayer model we find the simple result that the total acoustic impedance calculated without slip can be mapped to the total acoustic impedance allowing for slip by a simple replacement rule for the first layer,

$$Z_1 \rightarrow \frac{Z_1}{1 + s_1 Z_1} \quad (30)$$

The essential idea in introducing slip is that a discontinuity in the speed occurs so that the speeds obtained by approaching the device-layer one interface from either side no longer match. Hayward and Thompson^{24,25} have used a slip boundary condition in a multilayer system, but their solution involves simply scaling one speed by a complex slip factor. This type of approach has several limitations. Each interface involves a complex slip factor and hence two parameters. More importantly, the relationship of the slip factor to material and drive parameters, such as the shear modulus, layer thickness and density, and oscillation frequency are not well-defined within the approach. In the Stoke's law approach, the effect of Eq. (29) on the speeds at the device-layer one interface is to introduce a mis-match of,

$$v_1(z=0) = \frac{\dot{q}_s}{1 + s_1 Z_1} \quad (31)$$

Using Eq. (31) as the defining slip boundary condition for a single layer device will recover the result of Eq. (30). The advantage of this boundary condition is that material and drive parameters are introduced in a well-defined manner by the acoustic impedance calculated from the no-slip problem. In effect, Eq. (31) provides a definition of the complex slip parameters used by Hayward and Thompson^{24,25} through the single real parameter, s_l . When slip is weak, s_l is small and the mis-match in speeds vanishes, thus recovering the no-slip boundary condition. When slip is strong, s_l is large and the speed of the layer vanishes so that the layer is decoupled from the underlying motion of the substrate. It is worth cautioning that this last statement is a simplified interpretation as the layer impedance is a complex number involving a $\tanh()$ function with a complex argument. In essence, Eq. (31) can be viewed as introducing a first order approximation using a single-loop negative feedback system with a forward element of Z_l (the open-loop term) and a feedback term of s_l as shown in Fig. 2.

III. Results and Discussion

IIIa. Viscoelastic overlayer with no-slip boundary condition

Eqs. (13) and (17), for a device coated with a single layer of viscoelastic material, provide two complementary views of the acoustic impedance. For small relaxation times where the relaxation time is the ratio of the viscosity to high frequency shear modulus, the effective penetration depth reduces to the penetration depth and the Kanazawa and Gordon result for Newtonian liquids is recovered from Eq. (17). For large relaxation times and small argument (phase angle) in the $\tanh()$ function of Eq. (13) we recover the Sauerbrey result for mass loading by a thin rigid mass film. In the case that the argument of the $\tanh()$ function is not small the acoustic impedance provides a method of measuring the shear modulus of the film³¹. In examining thick films care is needed as the argument of the $\tanh()$ function is complex and this can lead to damped shear wave resonances. Experimentally, locating these resonances is one method by which the shear modulus of a film can be determined¹⁶. One consequence of the physical basis presented in this work is that the unified interpretation provided for QCMs,

which typically operate in the 1-10 MHz range, and SH-SAW devices, which can operate in the 100 MHz to GHz range, allows a wider frequency range to be investigated.

In Figs. 3 and 4 we use a Maxwell model with a single relaxation time to show the generic changes in acoustic impedance that can be expected as the layer thickness and viscoelasticity are altered. The normalised impedance $Z_{norm} = Z_f / \sqrt{\omega \rho_f \eta_f}$ depends on only two parameters $\omega\tau$ and t_f/δ . For Newtonian liquids, which have $\omega\tau$ small, both real and imaginary parts of the impedance increase with film thickness until a saturation occurs after a few penetration depths. For these thick Newtonian films the impedance is only sensitive to the properties of the liquid at the device interface; in this regime a device could also be used to sense the area of interface covered by the liquid. As $\omega\tau$ increases the influence of viscoelasticity increases, the effective penetration depth $\bar{\delta}$ lengthens and oscillations occur in the impedance. For very large relaxation times the liquid appears as an amorphous solid and the oscillations take on the character of sharp shear wave resonances, indicating the ability of the shear waves to travel to the free film surface, to reflect and interfere constructively. In this amorphous solid limit and for very thin films ($h/\delta \ll 1$) the real part of the acoustic impedance (energy dissipation) vanishes and only energy storage (imaginary part of the impedance) occurs. This corresponds to the Sauerbrey equation for rigidly coupled mass in which frequency decreases (i.e. positive $\text{Im}[Z_f]$) occur without loss of quality of the resonance. In assessing whether changes in the response of an acoustic wave device, such as a QCM, are due to changes in the viscoelasticity of the film it is necessary to compare the trends in the energy loss with those of the energy storage²⁹. For films much thinner than the viscous penetration depth increasing viscoelasticity results in decreases in the resonant frequency and a broadening of the resonance (see Fig. 4 and Fig. 5). For films much thicker than the penetration depth the frequency will increase back towards the unloaded resonant frequency as the viscoelasticity increases, but the attenuation initially increases and then decreases, so a broadening is followed by a sharpening of the resonance. In the region between these two

limits, it is possible to find a decreasing resonant frequency (i.e. $\text{Im}[Z_f]$ positive and becoming larger) and a sharpening of the resonance (i.e. $\text{Re}[Z_f]$ positive and becoming smaller) as $\omega\tau$ increases from 1 to 4. It is important to emphasise that changes in viscoelasticity of a film can, in principle, lead to all four combinations of increasing/decreasing resonant frequency and increasing/decreasing attenuation. It is also worth noting that extreme viscoelasticity may even result in a resonant frequency higher than the unloaded device as shown by the change in sign in Fig. 4.

IIIb. Slip at the substrate interface

For an acoustic wave device with a single layer we would expect slip to simply decouple the motion of the substrate from the layer. In order to assess whether this might occur an order of magnitude estimate for the slip parameter, s_l , is useful. This parameter occurs in Eq. (31) in a combination $(1+s_l Z_l)$ and we therefore anticipate that s_l will have dimensions of inverse impedance. Moreover the slip parameter must be related to both the layer and the device substrate and so a possible candidate is,

$$s_l = \frac{1}{\chi Z_{c1}} \quad (32)$$

where $Z_{c1} = \sqrt{\rho_l G_l}$ is the characteristic impedance of the layer and χ is a co-efficient of friction. For a glassy layer with $G_l \sim 10^9$ and $\rho_l = 1000 \text{ kg m}^{-3}$, $Z_{c1} \sim 10^6$ Rayls and taking a typical coefficient of friction of the order between 0.01 and 1 suggests that a slip parameter would have an order of magnitude of 10^{-5} to 10^{-7} . For a liquid, the characteristic impedance would be several orders of magnitude lower and the slip parameter would be correspondingly smaller. Normalising the impedance containing the slip factor (Eq. (30)) gives,

$$Z_{\text{slip-norm}} = \frac{Z_{\text{norm}}}{1 + \bar{s} Z_{\text{norm}}} \quad (33)$$

and this has a dependence on a parameter $\bar{s} = s \sqrt{\omega \rho_f \eta_f}$, which involves the frequency in addition to the two parameters $\omega\tau$ and t_f/δ . Using the density and viscosity of water and a 5 MHz oscillation frequency gives $\bar{s} \sim 5.6 \text{ s}$ whereas using the density and viscosity of a

10 000 cSt polydimethylsiloxane (PDMS) oil gives $\bar{s} \sim 1.8 \times 10^6 s$. In Figs. 7-10, we have chosen $\bar{s} = 0, 0.5$ and 1 to illustrate the structure of changes to the acoustic impedance that interfacial slip, within the model developed here, could produce; these values of \bar{s} are not intended to be taken as suggested values for experiments. For the Newtonian liquid in Figs. 7 and 8 our previous order of magnitude estimate of \bar{s} is far lower than 0.5. In contrast, for PDMS the estimate is consistent with an \bar{s} of the order of magnitude used in Fig. 9 and 10.

Figs. 7 and 8 show the effect of slip with $\bar{s} = 0, 0.5$ and 1 on a QCM device coated with a single layer of a Newtonian liquid (i.e. $\omega\tau=0$). For this layer, when the thickness is much greater than the viscous penetration depth, the effect of slip is to reduce the acoustic impedance in the manner anticipated by a decoupling of the liquid from the substrate. However, these curves show that the effect of slip is different when the film thickness is less than about one viscous penetration depth. In this case, the energy storage systematically decreases as slip increases, but in contrast the energy dissipation now increases rather than decreases. This model of slip may provide a basis for consideration of the effect of hydrophilic and hydrophobic surfaces and of surface roughness through their influence on the co-efficient of friction.

Figs. 9 and 10 show the effect of slip with $\bar{s} = 0, 0.5$ and 1 on a device coated with a single layer having an amorphous solid character (i.e. $\omega\tau=50$). Close to the shear wave film resonance, the effect of slip is to dampen and broaden the acoustic impedance. For thin films the effect of increasing slip is to increase the real part of the acoustic impedance and reduce the imaginary part. In this respect, the qualitative behaviour of thin films is the same whether the film is of a liquid or solid character although the slope of the imaginary part of the acoustic impedance with layer thickness changes to concave rather than convex. Whilst Figs. 9 and 10 only show the thin film limit, the thick film limit for an amorphous solid is similar to the Newtonian liquid thick film limit. The predicted behaviour of the thin amorphous solid

film is consistent with the experimental observations¹⁷ on sliding friction during the adsorption of a monolayer of Kr atoms on a gold electrode QCM at 80 K. Initially as atoms are adsorbed the frequency shift increases, but as the coverage becomes greater the frequency shift then decreases; this decreasing frequency shift is interpreted as a decoupling of the adsorbed atoms from the surface.

IIIc. Acoustic load concept

The treatment of interfacial slip in this paper has been based on the physical boundary condition at the substrate–first layer boundary and has used an approach based on mechanics. It is possible to interpret the results for slip in a single layer system (Eq. (30)) as arising from a generalised acoustic load. To do so we imagine a substrate coated with two layers, an infinitesimally thin intermediate layer with acoustic impedance Z_i immediately adjacent to the substrate and a second finite layer with acoustic impedance Z_1 . Assuming a no-slip boundary condition, Eq. (27) gives a total acoustic load for this double layer system of,

$$Z_L = \left(\frac{Z_i + Z_1}{1 + \frac{Z_i Z_1}{Z_{ci}^2}} \right) \quad (34)$$

This generalised acoustic load, Z_L , will give the same result as Eq. (30) obtained for a single layer of acoustic impedance Z_i , directly in contact with the substrate, but with a slip boundary condition, provided we choose,

$$Z_i = \left(\frac{Z_{ci} Z_1^2}{\chi_i Z_1^2 - Z_{ci} Z_1 - \chi_i Z_{ci}^2} \right) \quad (35)$$

where Z_{ci} is a characteristic impedance and χ_i is dimensionless “friction” coefficient. Thus, in this interpretation, slip generates a certain impedance for an intermediate layer. The concept of an intermediate, or boundary, acoustic impedance then allows for an additional magnitude and phase change of the propagating wave, which is presented as an additional magnitude and phase change of the overall acoustic load³².

III.d. Slip at intermediate interfaces in multilayer devices

How to include slip at intermediate interfaces, other than the device-layer one interface, in a multiple overlayer structure is not obvious as Stoke's law (Eq. (29)) does not easily generalise. At such an intermediate interface in a multilayer structure there are two boundary conditions, Eqs. (22) and (23), rather than the single boundary condition occurring at the device-layer one interface, Eq. (21). We can derive a solution where the speeds are discontinuous, but nonetheless keeping the continuity of the shear stress. The alternative formulation of Stoke's law involving a mismatch of the interface speeds (Eq. (31)) can be generalised to,

$$v_k \left(\sum_{p=1}^k t_p \right) = \frac{v_{k-1} \left(\sum_{p=1}^k t_p \right)}{1 + s_k Z_L} \quad (36)$$

where Z_L is the total load impedance of the k 'th and higher layers calculated using a no-slip boundary condition. One approximation to Z_L would be to sum the individual impedances of the $(n-k)$ top most layers. Whilst Eq. (36) is an obvious extension of Eq. (31) it is not the only choice that could be made. Alternatives include using the impedance of the k 'th layer calculated using a no-slip boundary condition in place of Z_L in the denominator in Eq. (36). It is likely that Eq. (36) will be a reasonable condition in a double layer system with slip at either of the two interfaces. Solving the model for two layers using the boundary conditions given by eqs. (21), (23), (24) and (36) gives the result,

$$Z_L = \left(\frac{Z_1 + Z_2}{1 + \frac{Z_1 Z_2}{\rho_1 G_1}} \right) \left(\frac{1 + s_2 Z_1 Z_2 / (Z_1 + Z_2)}{1 + s_2 Z_2 / \left(1 + \frac{Z_1 Z_2}{\rho_1 G_1} \right)} \right) \quad (37)$$

The first factor in the right hand side of Eq. (37) is the result for two-layers obtained using the no-slip boundary condition. The second factor is the correction allowing for slip. Examining Eq. (37), we find that it arises from the no-slip result for two layers using a simple replacement rule analogous to Eq. (30), i.e.

$$Z_2 \rightarrow \frac{Z_2}{1 + s_2 Z_2} \quad (38)$$

The consistency of the result in Eq. (37) with the result for a single-layer on a device can be checked by imagining the thickness of the first layer tends to zero. The result of Eq. (30) is then recovered. A second method of verifying the consistency is to imagine strong slip at the layer 1-layer 2 interface. The slip parameter s_2 then dominates the second factor in Eq. (37) and, after cancellations, Eq. (37) reduces to the acoustic impedance of the first layer. Physically, strong slip at this interface between the layers decouples the second layer and the device sees the same impedance as it would if it was covered by only a single layer. Using the single loop negative feedback view, illustrated in Fig. 2, the result for the two layer calculation suggests that slip at any layer, treated using the approximation represented by the slip boundary condition Eq. (36), will result in a replacement rule analogous to Eq. (38) with the index simply equal to the layer index k .

IV. Conclusion

A physical model for viscoelastic contributions to the sensor response of a range of acoustic wave devices has been developed in terms of the surface acoustic impedance. Results for a device with a single viscoelastic layer have been shown to contain the limits of rigid mass loading and loading by Newtonian liquids. The effects of the viscoelasticity on the effective viscous penetration depth and the development of shear wave resonances with increasing viscoelasticity have been illustrated. All four combinations of frequency increase/decrease and attenuation increase/decrease with changing viscoelasticity are shown to be possible. The extension of the model to multiple viscoelastic layers has been described and results explicitly derived for a two-layer system. These results are consistent with transmission line models of QCMs with two layers. The no-slip boundary condition at the interface between layers has been reconsidered. An alternative slip boundary condition based on a speed discontinuity related to the layer impedance calculated using a no-slip boundary condition has been introduced for a single layer system. For a system with a single thick layer, both liquid and

solid, slip reduces energy storage and energy loss whilst for thin liquid-like layers, slip can increase the energy loss. A generalized acoustic load concept has been introduced as an interpretation of the results for slip in a single layer QCM device. The inclusion of slip at any interface in a multiple layer system is more complicated and a possible modification of the boundary conditions has been suggested.

Acknowledgements

The authors gratefully acknowledge financial support from the UK Engineering and Physical Sciences Research Council (EPSRC) and from The British Council and DAAD.

References

- ¹ G. Sauerbrey, Z. Phys. **155**, 206 (1959).
- ² K. K. Kanazawa, J. G. Gordon, Anal. Chem. **57**, 1770 (1985).
- ³ S. Bruckenstein, M. Shay, Electrochim. Acta **30**, 1295 (1985).
- ⁴ E. M. Pater, S. Bruckenstein, and A. R. Hillman, J. Chem. Soc. Faraday Trans. **94**, 1097 (1998).
- ⁵ S. Ramirez and A. R. Hillman, J. Electrochem. Soc. **145**, 2640 (1998).
- ⁶ S. Rösler, R. Lucklum, R. Borngraber, J. Hartmann, and P. Hauptmann, Sensors and Actuators **B48**, 415 (1998).
- ⁷ J. M. Abad, F. Pariente, L. Hernandez and F. Lorenzo, Analytica Chim. Acta. **368**, 183 (1998).
- ⁸ E. Gizeli, M. Liley, C. R. Lowe, and H. Vogel, Anal. Chem. **69**, 4808 (1997).
- ⁹ S.P. Sakti, S. Rösler, R. Lucklum, P. Hauptmann, F. Bühling, and S. Ansorge, Sensors and Actuators, **76**, 98 (1999).
- ¹⁰ R. Lucklum, C. Behling, R.W. Cernosek and S.J. Martin, J. Phys. D: Appl. Phys. **30**, 346 (1997).
- ¹¹ R. W. Cernosek, S. J. Martin, A. R. Hillman, and H. L. Bandey, IEEE Trans. Ultrason., Ferroelect., Freq. Contr. **45**, 1399 (1998).
- ¹² H. L. Bandey, S. J. Martin, R. W. Cernosek, and A. R. Hillman, Anal. Chem. **71**, 2205 (1999).
- ¹³ C. Behling, R. Lucklum, and P. Hauptmann, Sensors and Actuators **A61**, 260 (1997).
- ¹⁴ M. Rodahl and B. Kasemo, Sensors and Actuators **A 54**, 448 (1996).
- ¹⁵ M. Voinova, M. Rodahl, M. Jonson and B. Kasemo, Physica Scripta **59**, 391 (1999).
- ¹⁶ G. McHale, M.K. Banerjee, M.I. Newton, V.V. Krylov, Phys. Rev B - Condens. Matt. **59**, 8262 (1999).
- ¹⁷ C. Mak, J. Krim, Faraday Discuss. **107**, 389 (1997).

- ¹⁸Dayo, W. Alnasrallah, J. Krim, Phys. Rev. Letts. **80**, 1690 (1998).
- ¹⁹M. Yang, M. Thompson and W.C. Duncan-Hewitt, Langmuir **9**, 811 (1993).
- ²⁰N. Schmitt, L. Tessier, F. Patat, J.M. Chovelon and C. Martelet, Sensors and Actuators **A46**, 357 (1995).
- ²¹L.M. Furtado, H. Su and M. Thompson, Anal. Chem. **71**, 1167 (1999).
- ²²S.J. Martin, G.C. Frye and A.J. Ricco, Anal. Chem. **65**, 2910 (1993).
- ²³S.J. Martin, Faraday Discuss. **107**, 463 (1997).
- ²⁴B. A. Cavic, F. L. Chou, L. M. Furtado, S. Ghafouri, G. L. Hayward, D.P. Mack, M.E. McGovern, H. Su, M. Thompson, Faraday Discuss. **107**, 159 (1997).
- ²⁵G.L. Hayward and M. Thompson, J. Appl. Phys. **83**, 2194 (1998).
- ²⁶C. Behling, R. Lucklum and P. Hauptmann, Meas. Sci. Technol. **A61** (1998) 1886-1893.
- ²⁷C. Behling, *The non-gravimetric response of thickness shear mode resonators for sensor applications*, PhD Thesis University of Magdeburg (1999).
- ²⁸R. Lucklum, C. Behling, and P. Hauptmann, Faraday Discuss. **109**, 123 (1997).
- ²⁹R. Lucklum, C. Behling, and P. Hauptmann, Anal. Chem. **71**, 2488 (1999).
- ³⁰R. Lucklum, C. Behling, and P. Hauptmann, IEEE Ultrason., Ferroel., Freq. Contr. (2000), in print.
- ³¹C. Behling, R. Lucklum, and P. Hauptmann, IEEE Ultrason., Ferroel., Freq. Contr. **46**, 1431 (1999).
- ³²R. Lucklum and G. McHale, 2000 IEEE/EIA Int. Freq. Contr. Symp., 7.-9.6.2000 Kansas City (MO).

Figure Captions

Figure 1 Three possible modes of oscillation of acoustic wave devices. The transverse waves in the QCM and SH-SAW devices and the longitudinal component of the Rayleigh SAW induce shearing of any viscoelastic overlayer.

Figure 1 - McHale et al (J. Appl. Phys.)

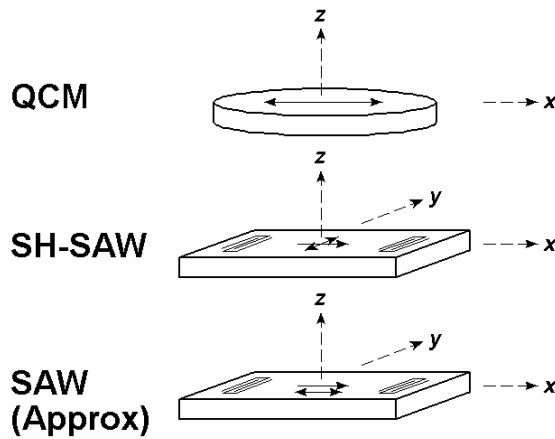


Figure 2 The effect of the slip boundary condition can be interpreted as a single-loop negative feedback system where the forward transfer is the impedance calculated with a no-slip boundary condition, Z_f , and the feedback block is s .

Figure 2 - McHale et al (J. Appl. Phys.)

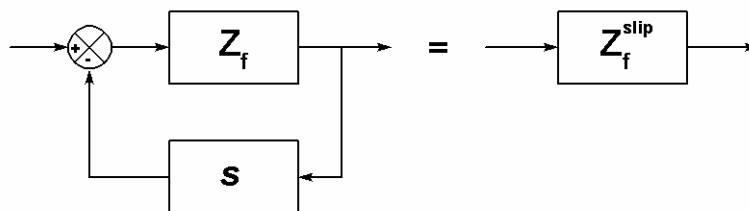


Figure 3 The change in the real part of the acoustic impedance of a single viscoelastic overlayer as a function of thickness and relaxation time using a Maxwell model. The transition in the nature of the film from liquid-like to amorphous solid is accompanied by the onset of shear wave resonances.

Figure 3 – McHale et al (J. Appl. Phys.)

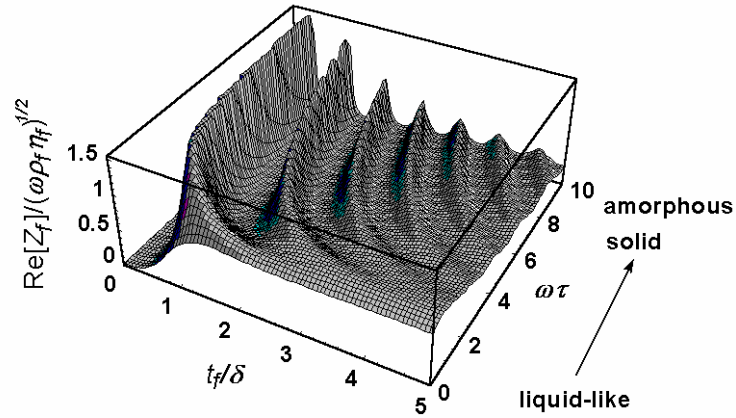


Figure 4 The change in the imaginary part of the acoustic impedance of a single viscoelastic overlayer as a function of thickness and relaxation time using a Maxwell model. The change in sign of the imaginary part of the film impedance indicates that frequencies larger than the unloaded resonant frequency can occur when devices are operated as resonators.

Figure 4 – McHale et al (J. Appl. Phys.)

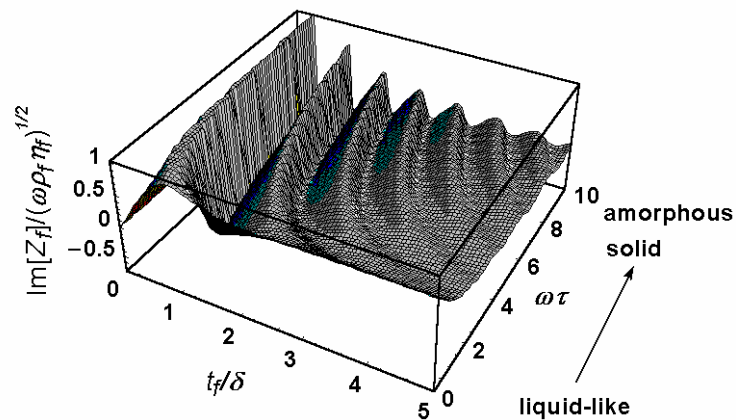


Figure 5 Changes in dissipation for $\omega\tau=0, 1$ and 4 (solid line, long dashes and short dashes, respectively). Increasing the relaxation time, and hence the viscoelasticity, increases the dissipation for thin films with thickness much less than the viscous penetration depth. However, for thicker films both increases and decreases can be seen.

Figure 5 – McHale et al (J. Appl. Phys.)

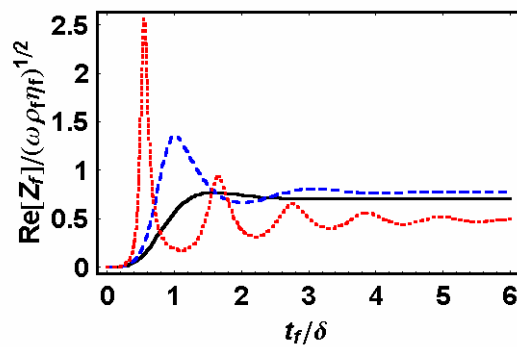


Figure 6 Changes in energy storage for $\omega\tau=0, 1$ and 4 (solid line, long dashes and short dashes, respectively). Depending on film thickness, it is possible to have frequency decreases or frequency increases as the relaxation time increases. In both cases, the corresponding changes in loss (Fig. 5) can be either increases or decreases depending on film thickness.

Figure 6 – McHale et al (J. Appl. Phys.)

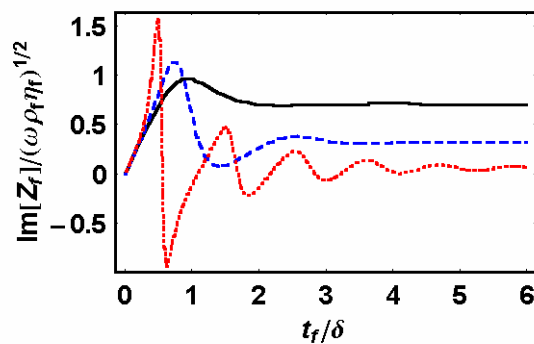


Figure 7 The real part of the film impedance for a single layer Newtonian liquid ($\omega\tau=0$) with slip parameters of $\bar{s} = 0, 0.5$ and 1 (solid line, long dashes and short dashes, respectively). For thick layers, slip decouples the fluid and the dissipation reduces. For thin layers slip can lead to increased dissipation.

Figure 7 – McHale et al (J. Appl. Phys.)

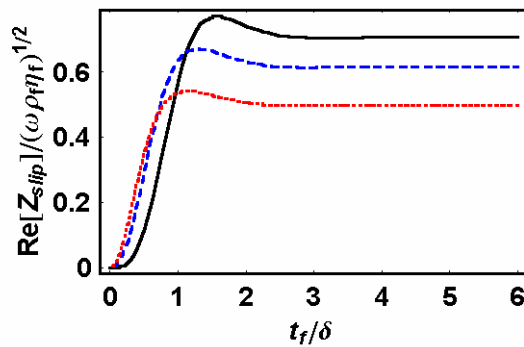


Figure 8 The imaginary part of the film impedance for a single layer Newtonian liquid ($\omega\tau=0$) with slip parameters of $\bar{s} = 0, 0.5$ and 1 (solid line, long dashes and short dashes, respectively). For thick layers, slip decouples the fluid and the frequency shift from the unloaded value reduces.

Figure 8 – McHale et al (J. Appl. Phys.)

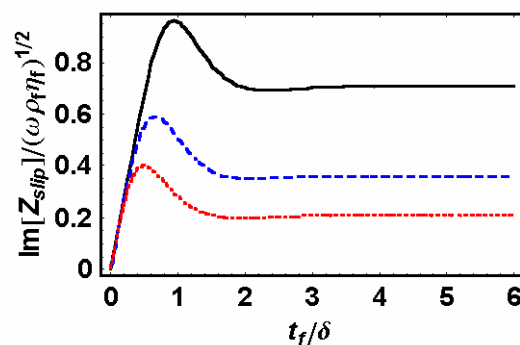


Figure 9 The real part of the film impedance for a single layer of an amorphous solid ($\omega\tau=50$) with slip parameters of $\bar{s} = 0, 0.5$ and 1 (solid line, long dashes and short dashes, respectively). The effect of slip is to reduce the amplitude and broaden the shear wave film resonance. For thin layers slip increases the dissipation.

Figure 9 – McHale et al (J. Appl. Phys.)

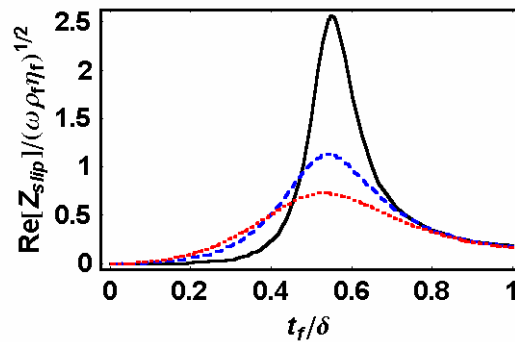


Figure 10 The imaginary part of the film impedance for a single layer of an amorphous solid ($\omega\tau=50$) with slip parameters of $\bar{s} = 0, 0.5$ and 1 (solid line, long dashes and short dashes, respectively). The broadening of the film resonance is evident. For thin layers increasing slip reduces the energy storage and hence the frequency shift.

Figure 10 – McHale et al (J. Appl. Phys.)

